Int. J. Electrochem. Sci., 14 **(2019)** 1197 – 1207, doi: 10.20964/2019.02.49

International Journal of
ELECTROCHEMICAL
SCIENCE
www.electrochemsci.org

Effects of Negative Electrodes Coated by ZnO with Different Morphologies on Electrochemical Performances and Safety of Lithium Ion Batteries

Chia-Ming Chang[1,3], *Hsiu-Fen Lin*[2,*], *Shih-Chieh Liao*[1], *Hsin-Tien Chiu*[3], *Chia-Erh Liu*[1] *and Han-Lin Guo*[2]

[1] Department of Nanomaterials for Energy Storage, Material & Chemical Research Laboratory, Industrial Technology Research Institute, Hsinchu 31040, Taiwan
[2] Department of Materials Science and Engineering, National Formosa University, Yunlin 64054, Taiwan
[3] Degree Program of Science, National Chiao Tung University, Hsinchu 30010, Taiwan
[*]E-mail: tiffany1030@nfu.edu.tw

Received: 6 October 2018 / *Accepted:* 21 November 2018 / *Published:* 5 January 2019

To improve the safety of lithium-ion batteries, this study applied topographically different ZnO to the surface of negative graphite electrodes to serve as heat-resistant layers and explored the effects of these layers on a battery's electrochemical and safety features. The results indicate that when using a tetrapod ZnO (T-ZnO) particle coating as a heat-resistant layer on a negative graphite electrode, ion diffusion is improved because T-ZnO has a three-dimensional network structure and forms highly porous layers. This causes batteries to retain excellent electrochemical characteristics even if they contain inactive substances. Moreover, the results of overcharge and penetration tests were satisfactory, suggesting that the batteries are highly safe.

Keywords: Tetrapod ZnO; Rod ZnO; Negative electrode; Electrochemistry; Safety; Thermal stability; Li-ion battery.

1. INTRODUCTION

Lithium-ion secondary batteries are employed in all types of electronics, such as laptops, mobile phones, tablets, cameras, and electric bicycles. They have become an indispensable part of our modern lives. To accommodate the needs of passenger aircrafts, hybrid vehicles, and electric vehicles, lithium-ion secondary batteries are being developed that are geared toward high energy density and high operating voltage. While trying to achieve these characteristics, safety issues are equally crucial [1-3]. In the past decade, several accidents have occurred that involved lithium batteries, such as those in

electric vehicles, aircraft laptops, and cell phones [4-7]. The explosion or ignition of a lithium-ion battery is usually caused by an internal short circuit [8], which results in local heat reactions and melts or contracts the battery's separator, leading to contact between the positive and negative electrodes while triggering a series of reactions and finally increasing the temperature [9-11].

Numerous methods have been reported for improving the thermal stability of batteries and thus enhancing battery safety and avoiding thermal runaway. Coating separators with ceramic powders such as SiO_2 [12], Al_2O_3 [13], ZrO_2 [14], and TiO_2 [15] can effectively prevent thermal shrinkage and mechanical breakdown. Cathodes may also be homogenously coated with inorganic nanoparticles to improve safety and electrochemical properties [16-21]. In addition, electrolyte additives have been used to reduce gas generation and mitigate flammability while providing overcharge protection [22-25]. However, few published studies [26-28] have discussed the safety of batteries containing negative electrodes with ceramic coatings.

In this present study, we used inorganic powders coated onto negative graphite electrodes as a heat-resistant layer. With this electrode, when thermal runaway occurs and the separator shrinks or melts, the heat-resistant coating isolates the positive electrode from the negative electrode, preventing contact between the two electrodes and thus a short circuit, ultimately reducing the loss of energy resulting from subsequent exothermic reactions. This study employed short-rod and tetrapod ZnO coatings on the surface of negative graphite electrodes and packed the electrodes into 18650 prismatic and pouch cells to examine their effects on battery safety and electrochemical characteristics.

2. EXPERIMENTAL

2.1 Preparation of ZnO particles

Nanosized short-rod ZnO (S-ZnO) particles of 99.5% purity were purchased from Sigma-Aldrich. Tetrapod ZnO (T-ZnO) particles were synthesized from a direct current plasma reactor. N_2 gas was employed as the plasma, the power of the plasma reactor was set as 70 kW, and zinc metal wires with a diameter of 1.2 mm (INNOVATOR SURFACE TECHNOLOGIES) were fed into the plasma flame at a fixed flow rate of 10 slm of carrier gas (i.e. air). Upon entering the plasma zone, the zinc powder immediately underwent vaporization, oxidation, and quenching to form ZnO, and the powder was collected in the bag filter of the reactor.

2.2 Fabrication of electrodes and lithium ion batteries

Positive electrodes were prepared by mixing 89 wt% $Li(Ni_{0.5}Co_{0.2}Mn_{0.3})O_2$ cathodes, 5 wt% acetylene carbon black, and 5 wt% poly-vinylidenefluoride (PVDF) into n-methyl-2-pyrrolidone (NMP) solution. The slurry was then coated onto aluminum foil. Negative electrodes were prepared similarly by mixing 90 wt% graphite (SLC-1520P), 1 wt% acetylene carbon black, and 9 wt% PVDF into the NMP solution before coating it onto copper foil. The ZnO particles were placed in a solvent mixture

(15/85, v/v) and uniformly dispersed through ball milling for 4 hours. This slurry was then spread using a slot die coating machine onto a negative electrode to act as a heat-resistant layer. Lithium-ion cells were assembled by sandwiching a separator between the positive electrode and the ZnO-coated negative electrode. The cells were then enclosed in stainless steel cases (18650) or pouch bags, and a certain amount of the liquid electrolyte, 1M $LiPF_6$ in ethylene carbonate and dimethyl carbonate (1:1 volume ratio), was injected.

2.3. Physical and electrochemical measurements

Morphology of the ZnO particles and ZnO-coated negative electrodes was examined using field emission scanning electron microscopy (SEM; Oxford, LEO 1530). The electrochemical performance was assessed by charging and discharging the cells at a current density of 0.16 A (0.1 C) with a voltage range of 2.7 to 4.2 V at room temperature. The electrodes were assembled in pouch cells and 18650 prismatic cells so as to study the penetration and overcharge properties, respectively.

3. RESULTS AND DISSCUSSION

3.1 Morphology of zinc oxide

SEM images of the crystal topography of S-ZnO and T-ZnO are displayed in Fig. 1. S-ZnO comprised short rods of 200 nm in length, whereas T-ZnO comprised tetrapod-shaped rods shorter than 100 nm and uneven in length. Top surface and cross-section images of the pristine, S-ZnO-coated, and T-ZnO-coated negative electrodes are presented in Fig. 2. A pristine negative electrode consisted of natural crystal graphite spheroids of length 13–16 μm and width 40 μm. Fig. 3 shows schematics of the negative electrodes coated with a ZnO heat-resistant layer; the thickness of both the S-ZnO and T-ZnO coatings was less than 2 μm. Fig. 3 illustrates how the short-rod-shaped crystals were piled up densely. Because of the unique 3D network structure of T-ZnO, this powder formed highly porous heat-resistant layers.

3.2 Effects of heat-resistant layers on electrochemical performance

Fig. 4 displays the charge–discharge curves of 18650 prismatic cells for a current density of 0.16 A (0.1 C) with a voltage range of 2.7–4.2 V at room temperature. The charge capacity of the cells assembled with the pristine, S-ZnO-coated, and T-ZnO-coated negative electrodes was 1.54, 1.55, and 1.56 Ah, respectively; the cells' reversible discharge capacity was 1.32, 1.23, and 1.33 Ah; and their coulombic efficiency was 85.7%, 79.3%, and 83.3%. The cells with the S-ZnO and T-ZnO coating layers had lower coulombic efficiency than those with the pristine electrode, possibly because ZnO is an inactive substance that mildly increases the irreversible capacity. The cell assembled with the S-ZnO-coated electrode had not only the poorest coulombic efficiency but also the lowest discharge capacity,

probably because the S-ZnO coating layer has a compact structure, which hinders lithium ions from entering and leaving, in turn affecting the performance of the cell.

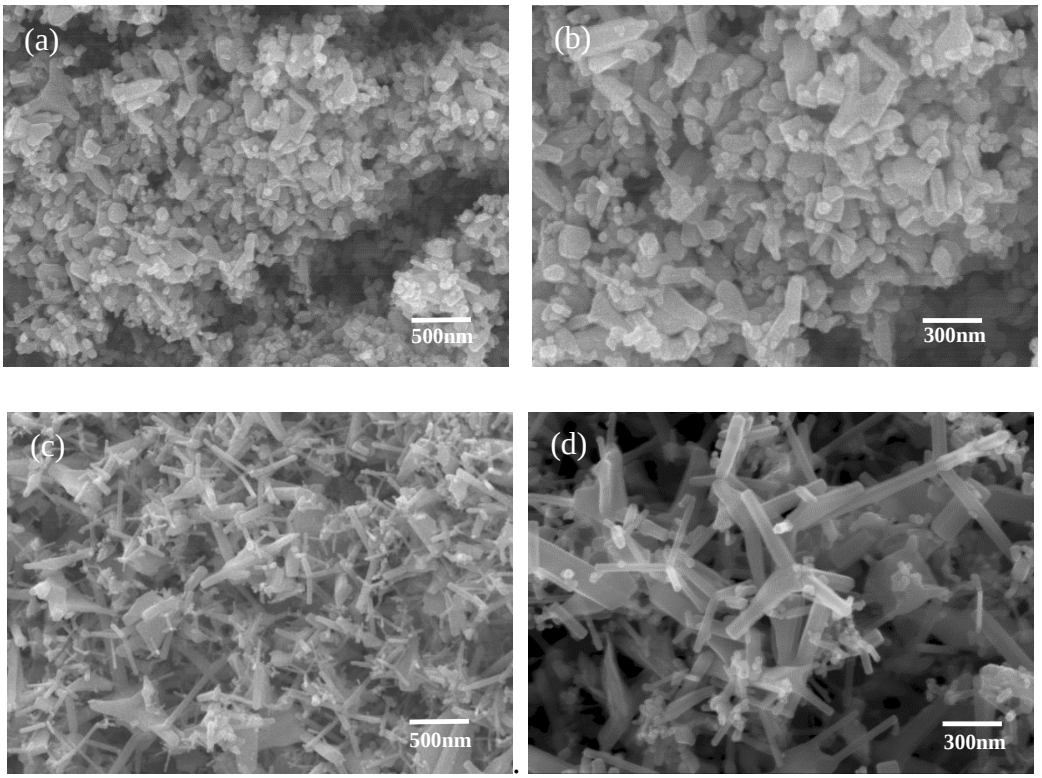

Figure 1. SEM images of (a), (b) S-ZnO and (c), (d)T-ZnO

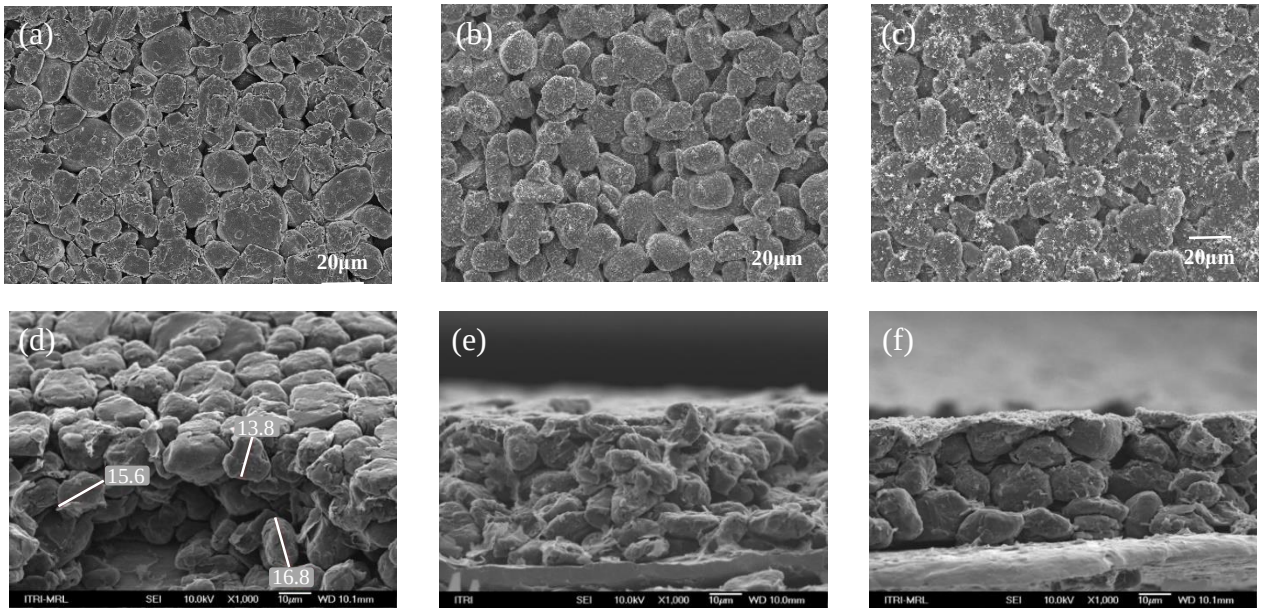

Figure 2. Top surface and cross-section morphology of (a),(d) pristine, (b),(e) S-ZnO-coated, and (c),(f) T-ZnO-coated negative electrodes.

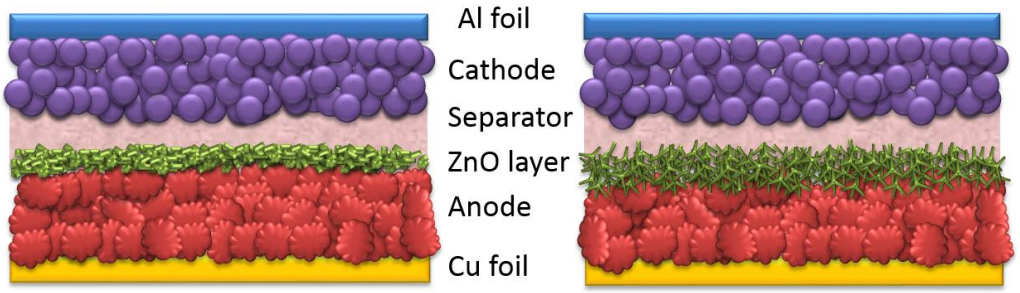

Figure 3. Schematics of the cells containing negative electrodes coated with (a) S-ZnO and (b) T-ZnO.

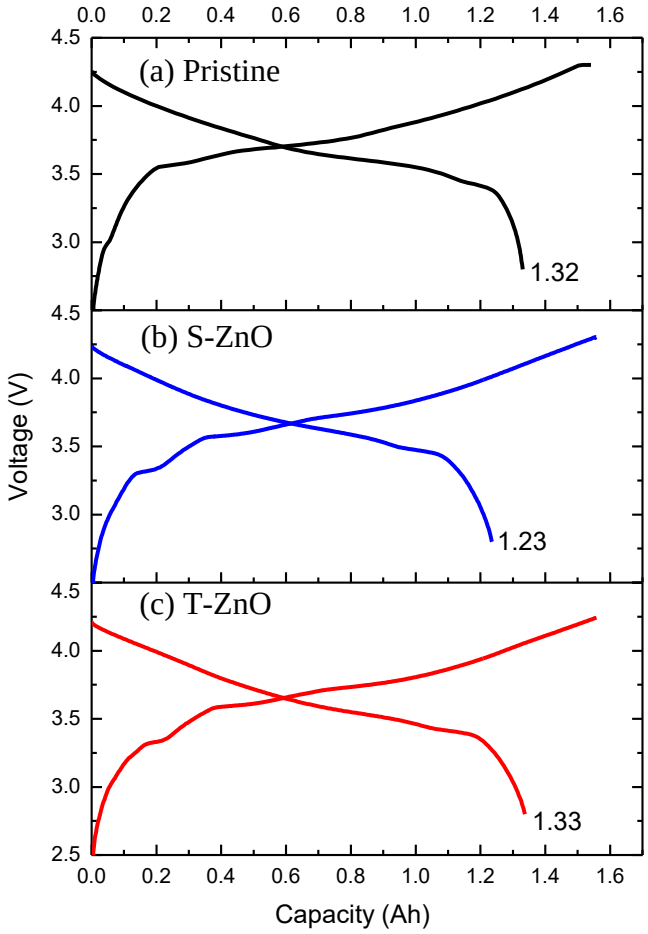

Figure 4. Charge–discharge curves of 18650 prismatic cells containing (a) pristine, (b) S-ZnO-coated, and (c) T-ZnO-coated negative electrodes.

To investigate the effect of the coated layers on cycle-life performance of the 18650 cells at high temperature, the cells containing pristine, S-ZnO-coated, and T-ZnO-coated negative electrodes were operated at a 0.5 C charge rate and 1 C discharge rate at 55 °C. The high-temperature cycle-life performance test results are illustrated in Fig. 5. The capacity retention of all three samples was higher than 90% during the first 100 cycles. However, when the capacity retention of the cells was 80%, the

cells containing the pristine, S-ZnO-coated, and T-ZnO-coated negative electrodes had undergone 160, 223, and 375 cycles, respectively. Jung et al. also discovered that Al_2O_3 coating the negative electrode improved the performance of the battery when cycling at high temperature [27] and high voltage [28]. It's due to the coating graphite electrode can reduce the formation of soluble byproducts [29], mitigating the coupled side reaction that accelerates degradation of the positive electrode. In this results, the cells containing ZnO coated shows the better cycle life at higher temperature than pristine and the T-ZnO-coated electrode shows the highest performance. This may have been due to the three-dimensional network of T-ZnO stabilizing the surface of the electrode, preventing the formation of SEIs after numerous cycles, or preventing lithium ions from forming deposits on the electrode surface during charges and discharges, in turn reducing degradation and the resistance increase rate.

.

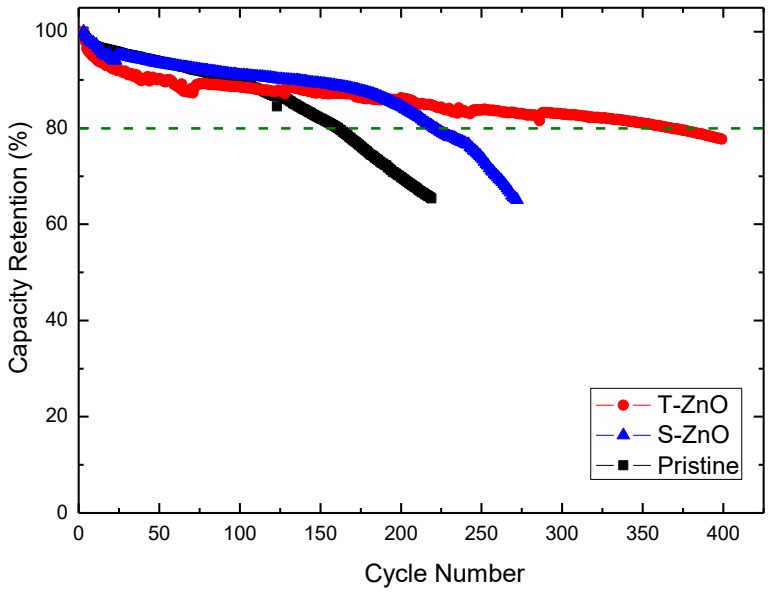

Figure 5. High-temperature cycle-life performance of 18650 prismatic cells containing pristine, S-ZnO-coated, and T-ZnO-coated negative electrodes.

3.3 Overcharge test of 18650 prismatic lithium-ion cells

Overcharging lithium-ion cells can lead to chemical and electrochemical reactions and trigger self-accelerating reactions in the batteries, which cause thermal runaway and potentially an explosion [30-35]. The 18650 cells containing pristine, S-ZnO-coated, and T-ZnO-coated negative electrodes were overcharged to 12 V, after which their voltage (green line) and the temperatures at the top (black line), middle (red line), and bottom (blue line) of the cells were measured.

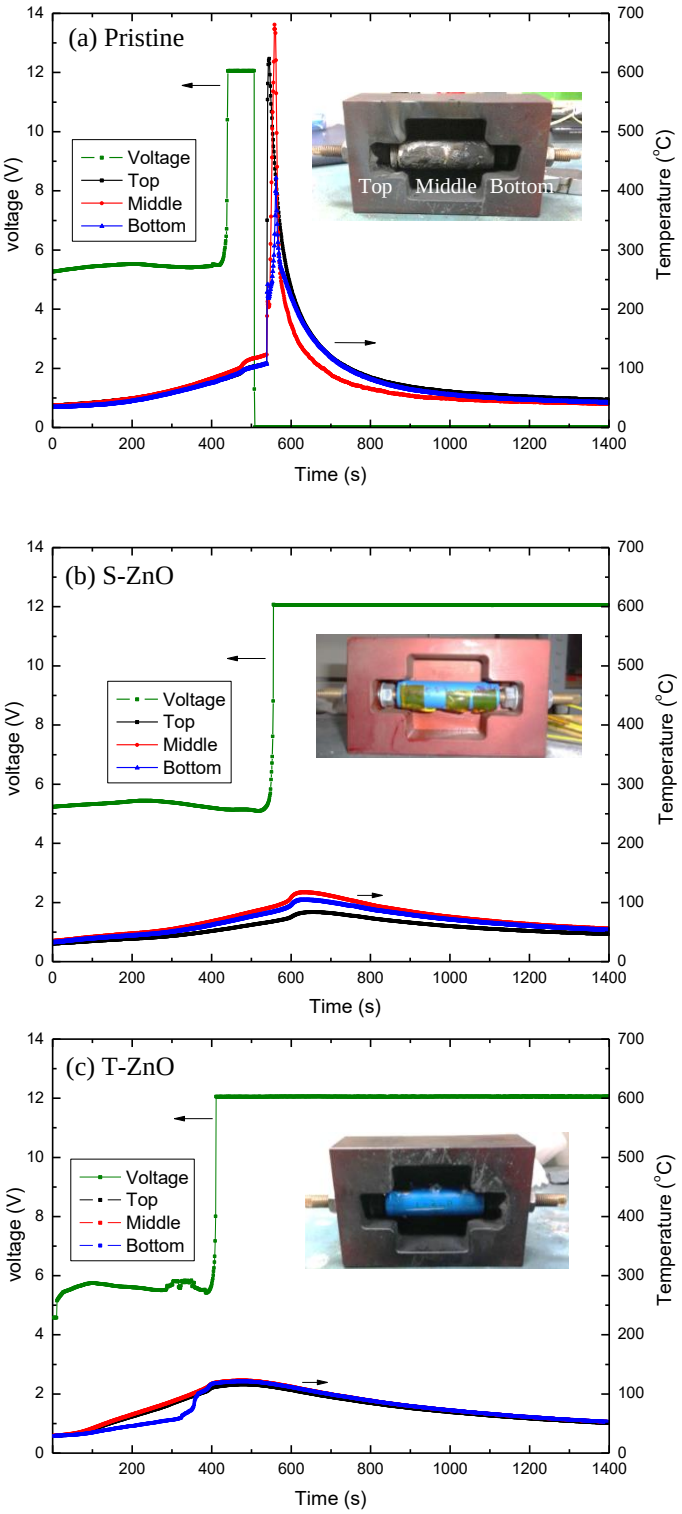

Figure 6. Voltage and temperature overlay plots of the results of overcharge test for 18650 cells containing (a) pristine, (b) S-ZnO-coated, and (c) T-ZnO-coated negative electrodes. Changes in voltage are shown as green lines and changes in temperature at the top, middle, and bottom of the cells are shown as black, red, and blue lines, respectively.

Fig. 6(a) shows the overcharge test result for the cell containing the pristine negative electrode. When the charging voltage reached 12 V, it was held for only 90 seconds, after which it dropped suddenly to 0 V. As the pristine cell heated up to higher than 165°C, the polypropylene–polyethylene–polypropylene separator began to shrink and melt [32], causing contact between the positive and negative electrodes and creating a series of exothermic reactions that caused the temperature to swiftly increase to 700°C. The thermal runaway of the cell caused evaporation of the electrolyte and an internal pressure increase, eventually causing fire and an explosion. The overcharge safety test results for the cells containing S-ZnO- and T-ZnO-coated negative electrodes are displayed in Fig. 6(b) and 6(c).

When the voltage reached and was then maintained at 12 V, the temperature of both cells first rose to 125°C and then dropped slowly to room temperature. At the completion of the tests, the S-ZnO- and T-ZnO-layer cells remained intact without any incidents of fire or explosions. According to the results of Jung et al. [27], the cell containing the Al_2O_3-coated negative graphite electrode generated significantly less heat. Thus, the solid electrolyte interphase (SEI) layer formed on the coated negative graphite electrode was smaller and more stable than that formed on the bare negative graphite electrode, which in turn dramatically affected the safety performance of the battery [34]. It can be demonstrated that when the negative electrode is coated with a ZnO heat-resistant layer, it can reduce exothermic reactions under high voltage (12V) and hold the cell's overall temperature at 125°C, not exceeding the melting point of the separator and thus preventing the cell from continual temperature increases; therefore, these layers increase the safety of lithium-ion batteries.

3.4 Penetration test of pouch cells

In penetration test [8, 36], both mechanical and electrical damage are induced in pouch cells. A blunt rod is forced through the cell to deform the electrode layers and eventually create a short circuit. First, the pouch cells were charged to 4.2 V and temperature sensors were attached to the top, middle, and bottom parts of the cells. The measured temperature changes are shown as black, red, and blue lines in Fig. 7, respectively. The fully charged pouch cells were placed into an explosion-proof box and crushed using a blunt nail of 2.5 mm diameter at a speed of 0.015 mm/s to cause microscale short circuits. The blunt nail was halted when the voltage difference of the cell dropped to 25 mV.

The results of penetration test for the pouch cell containing a pristine negative electrode are presented in Fig. 7(a). When the nail first touched the cell, the voltage dropped slightly. After the voltage difference had dropped to 25 mV, the nail was halted; the voltage dropped rapidly while the temperature increased drastically to 650°C, causing fire and an explosion. The penetration test initially caused minor local damage to the separator inside the cell, but the direct contact between the electrodes caused a series of thermal runaway reactions and complete short circuits, resulting in cell explosion and burning [8,31,36,37]. The results for the pouch cell containing the S-ZnO-coated negative electrode are shown in Fig. 7(b). After the nail halted, the top and bottom temperatures of the cell increased slowly to 90°C, whereas the temperature at the middle rose to 180°C because of the direct impact; concurrently, the voltage dropped to 0 V.

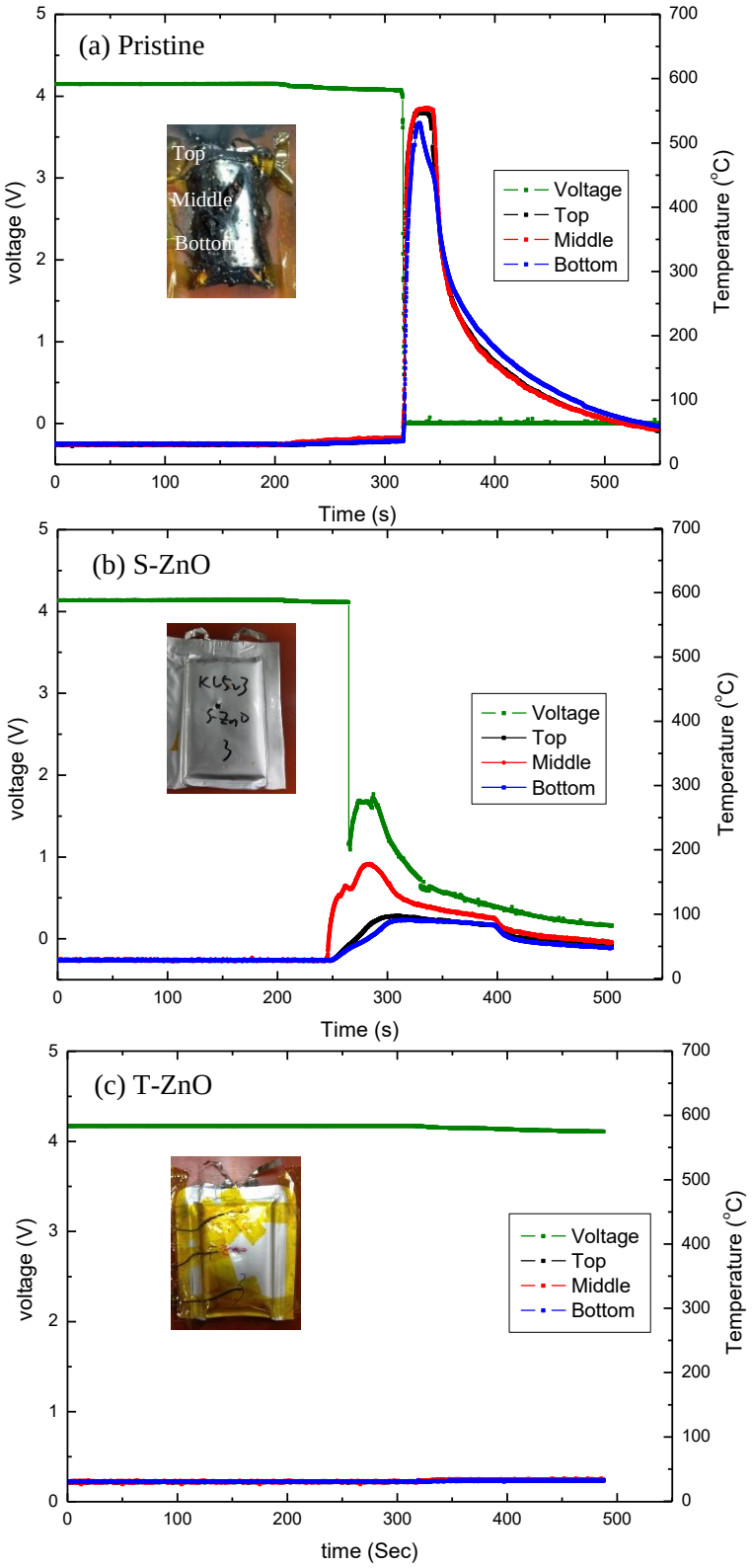

Figure 7. Voltage and temperature overlay plots of the results of penetration test for pouch cells containing (a) pristine, (b) S-ZnO-coated, and (c) T-ZnO-coated negative electrodes. Changes in voltage are shown as green lines and changes in temperature at the top, middle, and bottom of the cells are shown as black, red, and blue lines, respectively.

Although the higher temperature in the middle of the cell compared with the top and bottom would cause the separator to shrink, the S-ZnO layer acted as a barrier preventing direct contact of the positive electrode with the negative electrode and thus stopped a series of reactions that would have been triggered by a further thermal shock. The heat in the middle of the cell caused the cell containing the S-ZnO-coated electrode to expand but not explode. Fig. 7(c) presents the results for the pouch cell containing the T-ZnO-coated negative electrode. Once the nail had halted, the temperature increased gradually from room temperature to 70°C, stayed at this temperature for 300 seconds, and then cooled down. The voltage did not significantly decrease over time, and after the test, it was 3.5 V. After penetration test, we dismantled the battery and discovered that the nail's point had caused invasive damage to the cell, but cell failure had not occurred. The coating negative electrodes may protect the surface of the active powders in electrodes while maintaining an interparticle electronic pathway [27], besides, T-ZnO powder can adopt a three-dimensional protective structure when used to form a heat-resistant layer. The layer dissipates heat caused by microscale short circuits, having a strong positive impact on cell safety. In summary, batteries containing T-ZnO heat-resistant layers have excellent charge and discharge qualities while being highly safe.

4. CONCLUSIONS

This study employed T-ZnO-coated negative electrodes in batteries with a charge capacity of 1.56 Ah, reversible discharge capacity of 1.33 Ah, and coulombic efficiency of 83.3%. After undergoing 375 cycles at a high temperature of 55°C, the batteries had 80% capacity retention. In overcharge and penetration test, the T-ZnO heat-resistant layer was discovered to effectively prevent thermal shocks and enhance safety. These positive characteristics can be attributed to the three-dimensional network structure of the T-ZnO powder, with which a highly porous coating layer can be produced. This unique structure enables lithium ions to diffuse more quickly than they do in a dense heat-resistant layer, enabling construction of batteries, even if they contain inactive substances that retain high electrochemical performance.

ACKNOWLEDGMENTS
The authors appreciate the financial and technical support from Industrial Technology Research Institute and the Ministry of Science and Technology of the Republic of China (MOST 107-2635-E-150-001).

References

1. N.S. Choi, Z. Chen, S.A. Freunberger, X. Ji, Y.K. Sun, K. Amine, G. Yushin, L.F. Nazar, J. Cho and P.G. Bruce, *Angew. Chem., Int. Ed.*, 51 (2012) 9994.
2. J. B. Goodenough and K.-S. Park , *J. Am. Chem. Soc*., 135 (2013) 1167.
3. J.W. Wen, Y. Yu and C.H. Chen, *Mater. Express,* 2 (2012) 197.
4. G.P. Beauregard, Report of investigation: hybrids plus plug in hybrid electric vehicle, U.S. National Rural Electrical Cooperative Association (NRECA) and the U.S. Department of Energy, Idaho National Laboratory, (2008) Pwhoenix AZ, USA.

5. G. Back, Chevrolet volt battery incident overview Report (NHTSA Report DOT HS 811 57), U.S. Office of Vehicle Safety Compliance, (2012) Washington, DC, USA.
6. National Highway Traffic Safety Board, Auxiliary Power Unit Battery Fire Japan Airlines Boeing 787-8 (NTSB/AIR-14/01), (2014) Washington DC, USA.
7. N. Goto, Aircraft serious incident investigation report (AI2014-4), Japan Transport Safety Board, (2014) Tokyo, Japan.
8. X. Feng, M. Ouyang, X. Liu, L. Lu, Y. Xia and X. He, *Energy Storage Mater.,* 10 (2018) 246.
9. Q. Wang, P. Ping, X. Zhao, G. Chu, J. Sun and C. Chen, *J. Power Sources,* 208 (2012) 210.
10. P.G. Balakrishnan, R. Ramesh and T.P. Kumar, *J. Power Sources,* 155 (2006) 401.
11. E.P. Roth, D. H. Doughty and D. L. Pile, *J. power Sources,* 174 (2007) 579.
12. P. Zhang, L. Chen, C. Shi, P. Yang and J. Zhao, *J. Power Sources,* 284 (2015) 10.
13. S. Chuan , Z. Peng , C. Lixiao , Y. Pingting and Z. Jinbao, *J. Power Sources,* 270 (2014) 547.
14. W. Xiao, Y. Gong, H. Wang, L. Zhao, J. Liu and C. Yan, *Ceram. Int.,* 41 (2015) 14223.
15. Y. Xi, P. Zhang, H. Zhang, Z. Wan, W. Tu and H Tang, Int. *J. Electrochem. Sci.,* 12 (2017) 5421.
16. J. Cho, Y.- W. Kim, B. Kim, J.- G. Lee and B. Park, *Angew. Chem. Int. Ed.,* 42 (2003) 1618.
17. M.W. Anna, B. Chunmei, N.W. Johanna, M. Sumohan , S.C. Andrew , Z. Wu, Z. Li, M.S. Whittingham, K. Xu, S.M. George and M.F. Toney, *Chem. Mater.,* 27 (2015**)** 6146.
18. J. Cho, Y.J. Kim, T.-J Kim and B. Park, *Chem. Mater.,* 13 (2001) 18.
19. I.D. Scott, Y.S. Jung, A.S. Cavanagh, Y. Yan, A.C. Dillon, S.M. George and S.-H. Lee, *Nano Lett.,* 11 (2011) 414.
20. J. Cho, Y.J. Kim, T.-J. Kim and B. Park, *Angew. Chem. Int. Ed. Engl.,* 40 (2001) 3367.
21. J. Cho, Y.J. Kim and B. Park, *Chem. Mater.,* 12 (2000) 3788.
22. Q. Wang, L. Feng and J. Sun, *Energies,* 9 (2016) 424.
23. J. Chen and J.R. Dahn, Electrochem. *Solid-State Lett.,* 8 (2005) A59.
24. Z. Chen and K. Amine, *Electrochem. Commun.,* 9 (2007) 703.
25. Z. Chen, Y Qin and K. Amine. *Electrochim. Acta,* 54 (2009) 5605.
26. E. M. Börger, E. Jochler, J. Kaufmann, R. Ramme, A. Grimm, S. Nowak, F. M. Schappacher, U. Rodehorst, A.-C. Voigt, S. Passerini, M. Winter and A. Börger, *J. Energy Storage,* 13 (2017) 304.
27. Y.S. Jung, A.S. Cavanagh, L.A. Riley, S.H. Kang, A.C. Dillon, M.D. Groner, S.M. George, and S.H. Lee, *Adv. Mater.,* 22 (2010) 2172.
28. Y.S. Jung, P. Lu , A.S. Cavanagh , C. Ban , G.H. Kim, S.H. Lee , S.M. George , S. J. Harris , and A.C. Dillon, *Adv. Energy Mater.,* 3 (2013) 213
29. D. Aurbach, *J. Power Sources,* 89 (2000) 206.
30. T. Ohsaki, T. Kishi, T. Kuboki, N. Takami, N. Shimura, Y. Sato, M. Sekino and A. Satoh, *J. Power Sources* 146 (2005) 97.
31. R.A. Leising, M.J. Palazzo, E.S. Takeuchi and K.J. Takeuchi, *J. Electrochem. Soc.* 148 (2001) A838.
32. R.A. Leising, M.J. Palazzo, E.S. Takeuchi and K.J. Takeuchi, *J. Power Sources* 97-98 (2001) 681.
33. H. Wang and M.-C. Chen, Electrochem. *Solid-State Lett.,* 9 (2006) A82.
34. J.J. Woo, Z. Zhang, N.L. Dietz Rago, W. Lu and K. Amine, *J. Mater. Chem.,* A1 (2013) 8538.
35. H. Yang, H. Bang, K. Amine, J. Prakash, *J. Electrochem. Soc.* 152 (2005) A73.
36. V. Ruiz, A. Pfrang, A. Kriston, N. Omar, P. V. den Bossche, L. Boon-Brett, *Renew. Sust. Energ. Rev.,* 81 (2018) 1427.
37. A. V Le, M. Wang, Y. Shi, D. J Noelle and Y. Qiao, *J. Phys. D: Appl. Phys.,* 48 (2015) 385501.